Cancer Science
Japanese Cancer Association JCA
Open Access

MicroRNA-155-5p promotes hepatocellular carcinoma progression by suppressing PTEN through the PI3K/Akt pathway

Xiao Fu,[1] Hongqing Wen,[1,2] Li Jing,[1] Yujuan Yang,[3] Wenjuan Wang,[1] Xuan Liang,[1] Kejun Nan,[1] Yu Yao[1] and Tao Tian[1]

[1]Department of Medical Oncology, The First Affiliated Hospital of Xi'an Jiaotong University; [2]Department of Respiratory, Third Hospital of Xi'an; [3]The third Department of Cardiology, Shaanxi Provincial People's Hospital, Xi'an, Shaanxi, China

Key words

Hepatocellular carcinoma, hepatocellular carcinoma progression, microRNA-155-5p, PI3K/Akt pathway, PTEN

Correspondence

Tao Tian, Department of Medical Oncology, The First Affiliated Hospital of Xi'an Jiaotong University, 277 Yanta West Road, Xi'an, Shaanxi, China.
Tel: +86-13572206784; Fax: +86-29-85324086;
E-mail: tiantao0607@163.com
and
Yu Yao, Department of Medical Oncology, The First Affiliated Hospital of Xi'an Jiaotong University, 277 Yanta West Road, Xi'an, Shaanxi, China. Tel: +86-13572101611; Fax: +86-29-85324086; E-mail:13572101611@163.com

Funding Information

Natural Science Foundation of China (NO. 81301909 and NO. 81502099); the International Cooperation Project in Science and Technology of Shaanxi Province (NO. 2016KW-017).

Received August 26, 2016; Revised January 17, 2017; Accepted January 24, 2017

Cancer Sci **108** (2017) 620–631

doi: 10.1111/cas.13177

MicroRNA-155-5p (miR-155-5p) has been reported to play an oncogenic role in different human malignancies; however, its role in hepatocellular carcinoma (HCC) progression is not clearly understood. In this study, we used real-time PCR in 20 rats with chemically-induced HCC, 28 human HCC tissues, and the matched paracarcinoma tissues, and HCC cell lines to determine the expression patterns of miR-155-5p and PTEN mRNA. Algorithm-based and experimental strategies, such as dual luciferase gene reporter assays, real-time PCR and western blots were used to identify PTEN as a candidate miR-155-5p target. Gain- and loss-of-function experiments and administration of a PI3K/Akt pathway inhibitor (wortmannin) were used to identify the effects of miR-155-5p and PTEN in MTT assays, flow cytometric analysis, wound healing assays and transwell assays. The results showed that miR-155-5p was highly overexpressed; however, PTEN was underexpressed in the HCC rat models, human HCC tissues and cell lines. In addition, miR-155-5p upregulation and PTEN downregulation were significantly associated with TNM stage ($P < 0.05$). Through *in vitro* experiments, we found that miR-155-5p promoted proliferation, invasion and migration, but inhibited apoptosis in HCC by directly targeting the 3′-UTR of PTEN. Western blots showed that miR-155-5p inactivated Bax and caspase-9, but activated Bcl-2 to inhibit apoptosis, and it activated MMP to promote migration and invasion via the PI3K/Akt pathway. A xenograft tumor model was used to demonstrate that miR-155-5p targets PTEN and activates the PI3K/Akt pathway *in vivo* as well. Our study highlighted the importance of miR-155-5p and PTEN associated with aggressive HCC both *in vitro* and *in vivo*.

Hepatocellular carcinoma (HCC) is the sixth most common malignancy and the second leading cause of cancer-related death in the world, particularly in South-East Asia, including China, Korea and Japan, and sub-Saharan Africa.[1,2] Unfortunately, due to the asymptomatic lesions in the early stages, HCC patients are often diagnosed at an advanced stage, resulting in a poor prognosis. An understanding of the mechanisms of malignant progression of HCC may provide novel diagnostic biomarkers or therapeutic targets for patients with advanced HCC.

Phosphatase and tensin homolog deleted on chromosome ten (PTEN) is a major tumor suppressor gene, and its deletion, mutation or gene silencing has been reported in many cancers.[3–5] PTEN dephosphorylates phosphatidylinositol 3, 4, 5-triphosphate (PIP3) and decreases the activity of class I phosphatidylinositol 3-kinases (PI3K) that mediate growth and survival factor signaling through PI3K effectors such as Akt and mTOR.[3] Our previous studies demonstrated that PTEN regulated angiogenesis and VEGF expression in HCC[6] and inhibited migration and invasion of HepG2 cells.[7] Until recently, subtle decreases in gene dosage or protein activity of PTEN, especially post-transcriptional regulation, were attributed with tumorigenesis.[8]

MicroRNA (miR) are small (19–22 nucleotides [nts]) RNA molecules and play crucial functions in the regulation of important processes, such as development, proliferation, differentiation, apoptosis and stress responses.[9] Among these, miR-155 is a well-characterized miR and has been proven to participate in inflammatory responses,[10] immune system regulation,[11] hematologic system disorder,[12] cardiovascular diseases[13] and tumorigenesis.[14–18] MiR-155 is located on human chromosome 21q21.3 and was first identified as a frequent integration site of the avian leucosis virus.[19] Emerging evidence revealed that miR-155 was upregulated in human HCC tissues as well as in early stages of hepatocarcinogenesis in established animal models,[20] and could predict poor survival following liver transplantation.[21] Moreover, most recent research has indicated that miR-155 is involved in epithelial cell adhesion molecule-positive tumor cells in HCC.[22] However, little is known about the regulatory role of miR-155-5p

on PTEN in HCC progression. In this study, we found that miR-155-5p was upregulated, while PTEN was downregulated in a chemically-induced rat HCC model, and HCC tissue specimens. Both the expressions of miR-155-5p and PTEN were correlated with TNM stage. We confirmed PTEN as a novel target of miR-155-5p using dual luciferase reporter gene assays, real-time PCR, and western blots. Finally, we found that miR-155-5p increased proliferation, invasion and migration, but inhibited apoptosis *in vitro*; it promoted tumorigenesis *in vivo* in HCC through targeting PTEN and activation of the PI3K/Akt pathway.

Materials and Methods

Human tissue specimens. All protocols were approved by the Ethics Committee of Xi'an Jiaotong University, and informed consent was obtained from all patients before surgery. We obtained HCC tissues and paracarcinoma liver tissues of 28 patients who underwent surgery for HCC in the Department of Hepatobiliary Surgery at The First Affiliated Hospital of Xi'an Jiaotong University from January 2011 to February 2013. None had received chemotherapy or radiotherapy before surgery. HCC tissues and paracarcinoma liver tissues (>20 mm distant from the HCC) were fixed in 4%–10% neutral buffered formalin immediately after surgical removal. Twenty-four hours later the tissues were dehydrated and embedded in low melting paraffin. All specimens were histopathologically identified as HCC and all HCC tissues were graded by the American Joint Committee on Cancer (AJCC) TNM staging system by pathologists in The First Affiliated Hospital of Xi'an Jiaotong University, who were blinded to the results. Total RNA was extracted from formalin fixed paraffin embedded (FFPE) HCC tissues using a miRNeasyFFPE Kit (QIAGEN, Hilden, Germany) according to the manufacturer's protocol.

Rat model of chemically-induced hepatocellular carcinoma. Eight-week-old male Sprague–Dawley rats were purchased from the Shanghai Experimental Animal Center and were housed in a pathogen-free facility at the Animal Center of Xi'an Jiaotong University and the establishment of a rat model of chemically induced HCC was performed as previously described. The tumor types of all specimens were confirmed by two independent pathologists.[23]

Xenograft tumor model. Twenty-four 6-week-old male BALB/c nude mice were divided into two groups (12 mice per group) and subcutaneously injected with 50 μL of 1.0×10^6 HepG2 cells or Hep3B cells combined with 50 μL of Matrigel (BD Biosciences, San Jose, CA, USA). When the tumor mass became palpable (at day 7 after injection), each group was then randomly divided into a control group (injecting angomiR NC for HepG2 cells or antagomiR NC for Hep3B cells) and an experimental group (injecting angomiR for HepG2 cells or antagomiR for Hep3B cells). The sequences of angomiR NC, angomiR, antagomiR NC and antagomiR are listed in Table 1. The injection was repeated three times every week for 2 weeks. The tumor volume was measured with a caliper three times per week using the formula: volume = length × width^2/2. At day 21, tumors were extracted and processed for real-time PCR and immunohistochemistry analysis.

All *in vivo* protocols were approved by the Institutional Animal Care and Use Committee of Xi'an Jiaotong University.

Cell culture and transfection. The human immortalized normal hepatocyte cell line (LO2) and HCC cell lines (SMMC7721, HepG2, Hep3B, MHCC97H and Bel7402) were purchased from the Institute of Biochemistry and Cell Biology, Chinese Academy of Sciences, Shanghai, China. All cells were cultured in DMEM (Hyclone, Marlborough, MA, USA), containing 10% FBS (FBS; Transgene, Beijing, China), with 100 IU/mL penicillin and 100 μg/mL streptomycin (Hyclone, USA) in a 5% CO_2 incubator at 37°C.

Table 1. MiR-155-5p interference and PTEN siRNA sequences

MiR-155-5p interference	Sequences (5′–3′)
MiR-155-5p mimics	5′-UUAAUGCUAAUCGUCAUAGGGGU-3′
	5′-CCUAUCACGAUUAGCAUUAAUU-3′
MiR-155-5p mimics NC	5′-UUCUCCGAACGUGUCACGUTT-3′
/PTEN siRNA NC	5′-ACGUGACACGUUCGGAGAATT-3′
MiR-155-5p inhibitor	5′-ACCCCUAUCACGAUUAGCAUUAA-3′
MiR-155-5p inhibitor NC	5′-CAGUACUUUUGUGUAGUACAA-3′
PTEN siRNA-1565	5′-GACGGGAAGACAAGUUCAUTT-3′
	5′-UGAUUCUUUAACAGGUAGCTT-3′
PTEN siRNA-1727	5′-GCUACCUGUUAAAGAAUCATT-3′
	5′-AUCAACUUGUCUUCCCGUCTT-3′
PTEN siRNA-1999	5′-GAUCUUGACAAAGCAAAUATT-3′
	5′-UAUUUGCUUUGUCAAGAUCTT-3′
AngomiR NC	5′-UUCUCCGAACUGUCACGUTT-3′
	5′-ACGUGACACGUUCGGAGAATT-3′
AngomiR	5′-UUAAUGCUAAUCGUGAUAGGGGU-3′
	5′-CCCUAUCACGAUUAGCAUUAAUU-3′
AntagomiR NC	5′-UUCUCCGAACUGUCACGUTT-3′
	5′-ACGUGACACGUUCGGAGAATT-3′
AntagomiR	5′-ACCCCUAUCACGAUUAGCAUUAA-3′

Table 2. Sequence-specific primers

Primers	Sequences (5′–3′)
miR-155-5p	Forward:5′-TTAATGCTAATCGTGATAGGGGT-3′†
PTEN	Forward:5′-GAGCGTGCAGATAATGACAAGGAAT-3′
	Reverse: 5′-GGATTTGACGGCTCCTCTACTGTTT-3′
GAPDH	Forward: 5′-GCACCGTCAAGGCTGAGAAC-3′
	Reverse: 5′- TGGTGAAGACGCCAGTGGA-3′

†The Uni-miR qPCR primer was included in the kit.

The sequences of miR-155-5p mimics, miR-155-5p mimics NC, miR-155-5p inhibitor, miR-155-5p inhibitor NC and PTEN siRNA are shown in Table 1. Cells were plated onto 6-well or 24-well plates and transfected using Turbo Fect (Thermo, NY, USA) according to the manufacturer's instructions.

Real-time quantitative RT-PCR. To quantitate miR-155-5p and PTEN expression, total RNA was extracted from HCC cell lines with Fast200 (Tiangen, Beijing, China). The isolated total RNA was reverse transcribed using a Mir-X MiRNA First-Strand Synthesis Kit (Clone Tech, Mountain View, CA, USA) for miR and Prime Script RT Master Mix (Takara, Kusatsu, Shiga, Japan) for mRNA according to the manufacturer's instructions. Relative expression of miR-155-5p and PTEN mRNA was calculated by the comparative cycle threshold (CT) method using the expression of U6 small nuclear RNA as the reference for miR and GAPDH as the reference for mRNA. Sequence-specific primers for miR-155-5p, U6, PTEN and GAPDH are shown in Table 2.

The quantity of miR and mRNA was measured using SYBR Premix Ex Taq II (Perfect Real Time, Takara, Japan). The reactions were performed on a Light Cycler (Bio-Rad IQ5, Hercules, CA, USA). The PCR conditions were 10 s at 95°C, followed by 40 cycles at 95°C for 5 s and 60°C for 20 s. The $2^{-\Delta\Delta CT}$ method was used for analysis.

Dual luciferase reporter gene assay. PmiR-PTEN-wild type (WT), pmiR-PTEN-mutant type (Mut) and pmiR-negative control (NC) plasmids were constructed by Gene Pharm (Shanghai, China). HepG2 and Hep3B cells were plated onto 24-well plates and cotransfected with 500 ng of pmiR-PTEN-WT, pmiR-PTEN-Mut, or pmiR-NC and 10 nM miR-155-5p mimics, inhibitor or negative control (NC) using Turbo-Fect. After 24 h co-transfection, cells were lysed by PLB buffer, and assayed by a Dual-Luciferase Reporter Assay System (Promega, Madison, WI, USA) according to the manufacturer's instructions. The tests were repeated in triplicate.

Cell apoptosis detection. Transfected cells were harvested 48 h after transfection. The apoptosis of transfected cells was quantified using an Annexin-V-7AAD Staining Kit (Key GENE BioTECH, Nanjing, Jiangsu, China) according to the manufacturer's protocol. The tests were repeated in triplicate.

Western blots. Transfected cells were harvested 48 h after transfection. Cells were lysed in RIPA buffer (Heart, Beijing, China). Total protein samples were separated by SDS-PAGE polyacrylamide gel and transferred onto a PVDF membrane (Millipore, Billerica, MA, USA). The membranes were immunological overnight at 4°C with primary antibodies as follows: PTEN (1:500; WanleiBio, Shenyang, Liaoning, China); Akt and phosphorylated-Akt (phosphoresce on S473; 1:500, Abcam, San Francisco, CA, USA); mTOR and phosphorylated-mTOR (phosphorylated on S2998; 1:1000, Bioworld, Nanjing, Jiangsu, China); Bax and Bcl-2 (1:1000, Cell Signaling, Danvers, MA, USA); caspase-9 (1:500, Protein Tech, Wuhan, Hubei, China); and human β-actin (1:5000; Transgene, China). PVDF membranes were washed with TBST and then incubated with a secondary antibody, HRP-conjugated goat IgG (1:5000; Transgene, China) for 1 h at 37°C. Signals were detected by the Bio-Rad Gel imaging system. The images were quantified by Quantity One (Bio-Rad, USA), and relative protein expression was normalized to β-actin levels in each sample. All experiments were performed in triplicate.

MTT assay. The proliferation of transfected cells was measured by MTT assay on FLUOstar OPTIMA (BMG). Cells were plated in 96-well plates 6 h after transfection (5×10^3/well), incubated for 24, 48 and 72 h, and assayed for absorbance at 492 nm. The data were summarized as mean ± SD from three independent trials.

Wound healing assay. HepG2 and Hep3B cells were seeded in 6-well plates. A total of 6 h after transfection (80% confluence), cell layers in serum-free medium were scratched with a sterile 200-μL pipette tip. After scratching, the debris was removed by washing with PBS. After 24 h incubation, 3 fields (10 ×) were randomly visualized to assess migration. All experiments were performed in triplicate.

***In vitro* transwell invasion assay.** Transwell membranes (Millipore, USA) coated with Matrigel and serum-free medium were used to assay cell invasion. At 6 h post-transfection, cells were cultured into 100-μL serum-free medium and reseeded into the upper chamber, and 500 μL of 20% FBS medium was added to the lower chamber as a chemoattractant. After 24 h of incubation, the invasive cells were fixed with 4% paraformaldehyde and stained with 0.1% crystal violet (Beyotime, Shanghai, China), and counted from five randomly-selected fields at 200 × magnification. Data were obtained from three independent experiments and are shown as mean ± SD.

Immunohistochemistry. The immunohistochemical staining of PTEN and p-Akt was performed as previously described.[6] The immunostaining results were scored as the percentage of cells staining positive as follows: 0 for <1% of cells, 1 for 1%–25% of cells, 2 for 26%–50% of cells, 3 for 51%–75% of cells and 4 for >75% of cells. Staining intensity was graded as follows: 0 for no staining; 1 for weak staining; 2 for moderate staining; and 3 for strong staining. The histological score (H-score) of PTEN and p-Akt for each section was computed using the following formula: H-score = ratio score × intensity score.

Statistical analysis. Data were presented as mean ± SD unless otherwise indicated and were compared using Student's *t*-test or one-way ANOVA. All analyses were performed with SPSS 19.0 (SPSS, Chicago, IL, USA), and a value of $P < 0.05$ was considered to indicate statistical significance.

Results

MiR-155-5p was upregulated and PTEN was downregulated in a chemically-induced hepatocellular carcinoma rat model, human hepatocellular carcinoma tissues and cells. We determined the expressions of miR-155-5p and PTEN mRNA in a rat model of HCC induced by diethylnitrosamine/N-nitrosomorpholine (DEN), which is similar to human HCC in terms of morphology and histology.[24] The tumor types of all specimens were confirmed by two independent pathologists.[23] Real-time PCR results showed that miR-155-5p was significantly upregulated in 19 HCC tissues, but PTEN mRNA was downregulated in 14

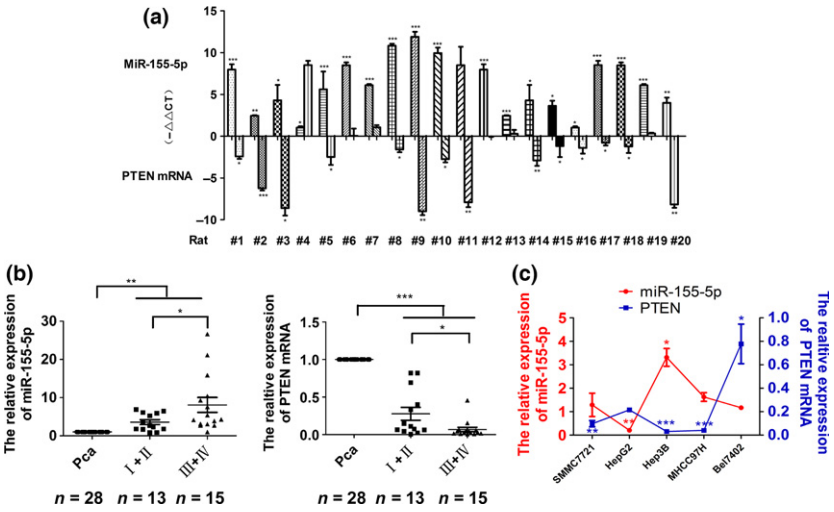

Fig. 1. The expression of miR-155-5p in hepatocellular carcinoma (HCC) tissues and cell lines. (a) The expression of miR-155-5p and PTEN mRNA in chemically-induced HCC rats, compared with normal liver tissues. $*P < 0.05$, $**P < 0.01$ and $***P < 0.001$ by Student's *t*-test. (b) The expression of miR-155-5p in various TNM stages, $*P < 0.05$, $**P < 0.01$ by Student's *t*-test, and PTEN mRNA in HCC tissues according to TNM stages, and paracarcinoma liver tissues. $*P < 0.05$, $***P < 0.001$ by Student's *t*-test. (c) Expression of miR-155-5p and PTEN mRNA in HCC cell lines versus the normal hepatic cell line LO2. *n* = three independent experiments, $*P < 0.05$, $**P < 0.01$, $***P < 0.001$ by ANOVA. Pca indicates matched paracarcinoma liver tissues.

Table 3. Correlation between clinicopathological features and the expression of miR-155-5p and PTEN in HCC

Characteristics	*n*	Percentage	MiR-155-5p relative expression (mean ± SD)	*P*	PTEN mRNA relative expression (mean ± SD)	*P*
Clinicopathological features				0.0***		0.0***
Adjacent non-cancerous liver tissues	28	100	1		1	
HCC	28	100	6.0 ± 6.0		0.2±0.3	
Age				0.09		0.9
≥55	11	40.3	8.4 ± 7.3		0.2 ± 0.8	
<55	17	60.7	4.4 ± 4.7		0.2 ± 0.3	
Gender				0.9		0.9
Male	22	78.6	6.9 ± 6.5		0.2 ± 0.3	
Female	6	21.4	2.8 ± 1.8		0.2 ± 0.2	
TNM				0.04*		0.04*
I + II	13	46.4	3.6 ± 2.2		0.3 ± 0.3	
III + IV	15	53.6	8.1 ± 7.5		0.07 ± 0.1	
Compliants				0.84		0.35
−	25	89.3	5.9 ± 6.3		0.2 ± 0.3	
+	3	10.7	6.7 ± 3.8		0.06 ± 0.06	
HBV				0.56		0.89
−	2	7.1	3.5 ± 1.1		0.4 ± 0.6	
+	26	92.9	6.2 ± 6.2		0.2 ± 0.2	
AFP (ng/mL)				0.65		0.65
≤20	9	32.1	4.8 ± 3.1		0.2 ± 0.3	
>20	19	67.9	5.7 ± 6.3		0.2 ± 0.3	
Cirrhosis				0.78		0.73
−	14	50.0	5.7 ± 4.5		0.2 ± 0.3	
+	14	50.0	5.1 ± 4.1		0.2 ± 0.3	

AFP, alpha-fetoprotein; HBV, hepatitis B virus; HCC, hepatocellular carcinoma; TNM, tumor-node-metastasis. *$P < 0.05$, ***$P < 0.001$.

HCC tissues from chemically-induced HCC rats, compared with normal rats ($P < 0.05$). ($-\Delta\Delta$CT) values of miR-155-5p and PTEN mRNA were obtained using U6 snRNA and GAPDH mRNA as an internal control, respectively, and the results are shown in Figure 1a.

To determine the expression of miR-155-5p in human HCC tissues, real-time PCR analysis was performed on 28 pairs of FFPE human primary HCC and matched paracarcinoma liver specimens. Compared with matched paracarcinoma tissues, miR-155-5p levels were significantly elevated (6.0-fold increase) in HCC tissues ($P < 0.01$). Moreover, its expression was significantly higher (8.1-fold increase) in stage III and IV HCC tissues (13 patients), compared with stage I and II HCC tissues (3.6-fold increase, 15 patients, $P < 0.05$). However, PTEN mRNA was significantly downregulated (0.2-fold decrease) in HCC tissues compared with matched paracarcinoma tissues ($P < 0.001$), and its expression was lower in stages III and IV HCC tissues (0.07-fold decrease), compared with stages I and II (0.3-fold decrease, $P < 0.05$, Fig. 1b). No significant association between miR-155-5p or PTEN mRNA expression level and patient age, gender, complaints, HBV affection, AFP level or cirrhosis was observed in any of the 28 HCC cases. The parameters of 28 HCC patients are summarized in Table 3.

Real-time PCR in HCC cell lines showed 1.29, 3.31 and 1.63-fold increases of miR-155-5p in SMMC7721, Hep3B and MHCC97H cells, respectively ($P < 0.05$). There was a 0.21-fold decrease in HepG2 cells ($P < 0.01$). The expression of PTEN mRNA was underexpressed in SMMC7721, Hep3B and MHCC97H cells (0.49, 0.16 and 0.20-fold decreases, respectively). However, PTEN mRNA was overexpressed in HepG2 and Bel7402 cells (1.08 and 3.89-fold increases, respectively, Fig. 1c). To further understand the biological effects of miR-155-5p, we chose Hep3B cells in which miR-155-5p was overexpressed, and HepG2 cells, in which miR-155-5p was underexpressed, to confirm the relationship between miR-155-5p and PTEN and to conduct loss-and gain-of-function experiments.

PTEN is a novel target of miR-155-5p. To determine whether miR-155-5p directly targeted the 3′-UTR of PTEN, 3′-UTR of PTEN was cloned into pmiR-Report luciferase reporter vectors (Fig. 2a). Cells were then co-transfected with miR-155-5p mimics, inhibitor or their respective negative control (NC) together with the luciferase reporter plasmids carrying the relevant wild (WT) or mutant (Mut) type 3′-UTR PTEN. Luciferase activity was measured and normalized to the luciferase activity in cells cotransfected with miR mimics NC and luciferase reporter carrying wild-type 3′-UTR PTEN. In Hep3B and HepG2 cells, the relative wild type of PTEN 3′-UTR luciferase activity was significantly lower in the presence of miR-155-5p mimics (62.40 ± 10.15% and 21.20 ± 10.74%, respectively; $P < 0.05$). Moreover, when the PTEN 3′-UTR was mutated (pmiR-PTEN-Mut), the decrease in relative luciferase activity was reduced in both Hep3B and HepG2 cells (96.51 ± 2.26% and 96.52 ± 1.40%, respectively). When miR-155-5p mimics or inhibitor together with the mutant type of PTEN 3′-UTR were co-transfected, the relative luciferase activity did not change significantly compared with co-transfected miR mimics NC and mutant type of PTEN 3′-UTR in both Hep3B and HepG2 cells (Fig. 2b).

After confirming transduction of the miR-155-5p inhibitor in Hep3B (Fig. S1), real-time PCR and western blots were used to further demonstrate a dose-dependent increase of PTEN in mRNA and protein levels, and a dose-dependent decrease of phosphorylated-Akt (p-Akt). In contrast, we also detected a

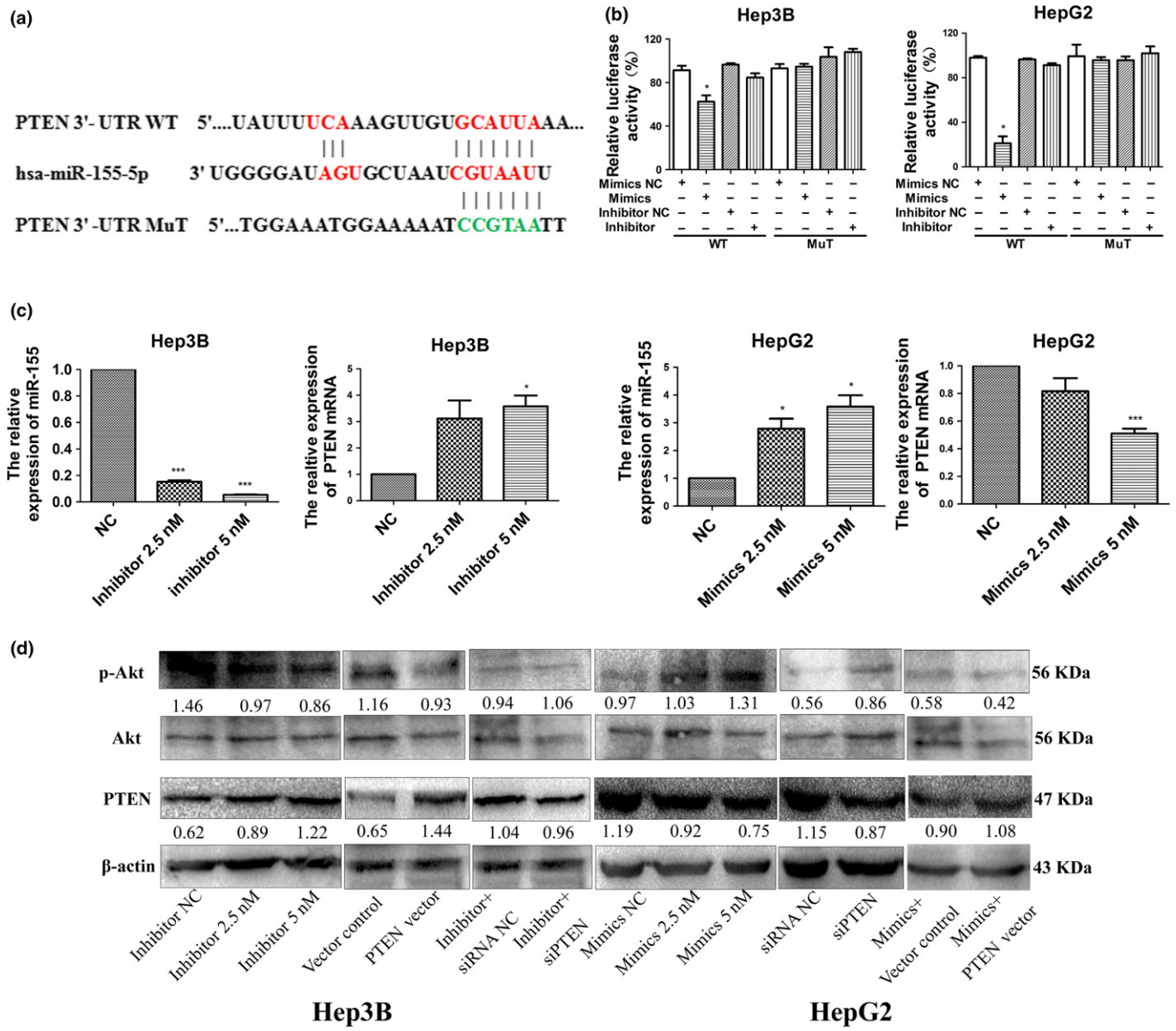

Fig. 2. PTEN is the target of miR-155-5p. (a) MiR-155-5p and its putative binding sequence in the 3′-UTR of PTEN. Mutant miR-155-5p binding sites were generated in the complementary site for the seed region of miR-155-5p (WT, wild type; Mut, mutant type). (b) MiR-155-5p effects on luciferase activity in cells that carried the wild type and mutant type 3′-UTR of PTEN. n = three repeats with similar results, $^*P < 0.05$ by Student's t-test. (c) The expression of miR-155-5p, and PTEN according to the dose of miR-155-5p inhibitor in Hep3B cells and mimics in HepG2 cells; n = three repeats with similar results; $^*P < 0.05$, $^{***}P < 0.001$ by Student's t-test. (d) The expression of PTEN and phosphorylation of Akt according to the dose of miR-155-5p inhibitor in Hep3B cells and mimics in HepG2 cells, the intensity of each band was quantified; the value under each lane indicates the relative expression level of the regulators; n = three repeats with similar results. p-Akt, phosphorylated Akt.

dose-dependent decrease in PTEN, and a dose-dependent increase in p-Akt when HepG2 cells were transfected with miR-155-5p mimics. Using western blots, we found that transfecting PTEN plasmid into Hep3B cells led to an increase of PTEN expression both in mRNA and protein levels, and a decrease in phosphorylation of Akt; the effects of transfecting PTEN siRNA into HepG2 cells resembled the effects of the miR-155-5p mimics. In addition, the expressions of PTEN and p-Akt were rescued by siPTEN in Hep3B cells transfected with the miR-155-5p inhibitor, and vice versa in HepG2 cells (Fig. 2c,d). Taken together, our results have demonstrated that miR-155-5p regulated PTEN expression at both the post-transcriptional and protein levels through targeting PTEN 3′-UTR.

MiR-155-5p promotes proliferation, migration, invasion and reduced apoptosis in hepatocellular carcinoma. In gain- and loss-of-function experiments to evaluate the effects of miR-155-5p in HCC malignancy, Hep3B and HepG2 cells were transfected with miR-155-5p inhibitor and mimics, respectively. MiR-155-5p depletion significantly decreased cell viability in Hep3B by 65.1%; in contrast, miR-155-5p overexpression increased cell viability in HepG2 by 20.8% at 48 h after transfection, compared with respective NC ($P < 0.01$; Fig. 3a). In addition, the results of flow cytometric analysis showed that in Hep3B cells, apoptosis changed from 2.99 ± 0.07% (when transduced inhibitor NC) to 5.77 ± 0.42% (when transduced miR-155-5p inhibitor, $P < 0.001$); in HepG2 cells, the apoptosis rate changed from

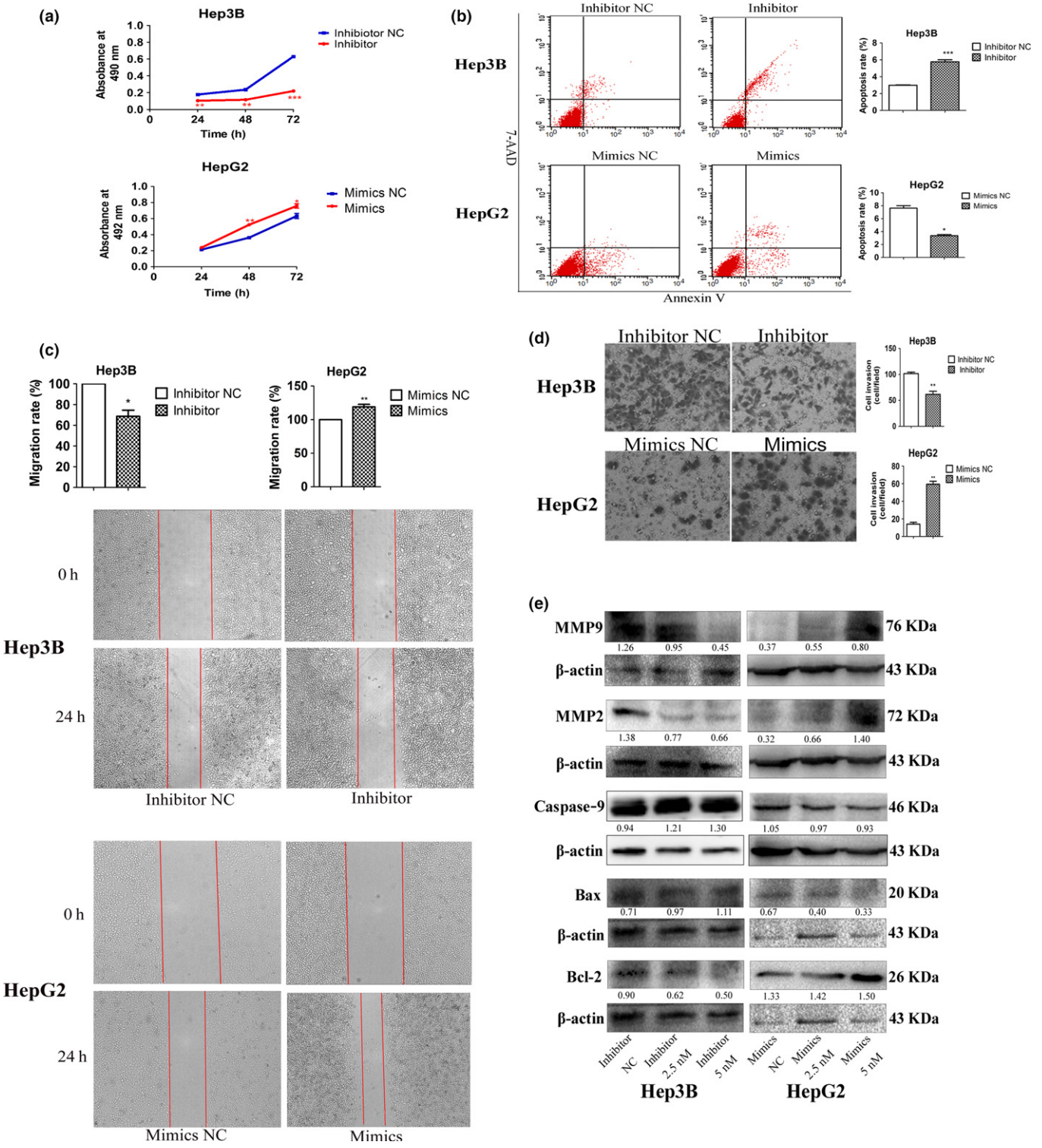

Fig. 3. The effects of miR-155-5p on hepatocellular carcinoma (HCC) cell proliferation, apoptosis, invasion and migration. (a–e) Cell viability, the percentage of apoptotic cells, wound healing and transwell assays, and the expression of Bcl-2, Bax, caspase-9, MMP2 and MMP9 in Hep3B and HepG2 transfected with miR-155-5p inhibitor and mimics, respectively; the intensity of each band was quantified; the value under each lane indicates the relative expression level of the regulators; *n* = three repeats with similar results; **P* < 0.05, ***P* < 0.01, ****P* < 0.001 by Student's *t*-test versus inhibitor and mimics NC, respectively.

7.63 ± 0.66% (when transduced mimics NC) to 3.37 ± 0.29% (when transduced miR-155-5p mimics, $P < 0.05$, Fig. 3b).

Given the strong correlation of miR-155-5p overexpression with aggressive HCC TNM stage, we investigated changes in cell migration and invasion after suppression or ectopic expression of miR-155-5p. According to the results of wound healing experiments, knocking down miR-155-5p in Hep3B cells reduced the ability of migration by 68.67%, but

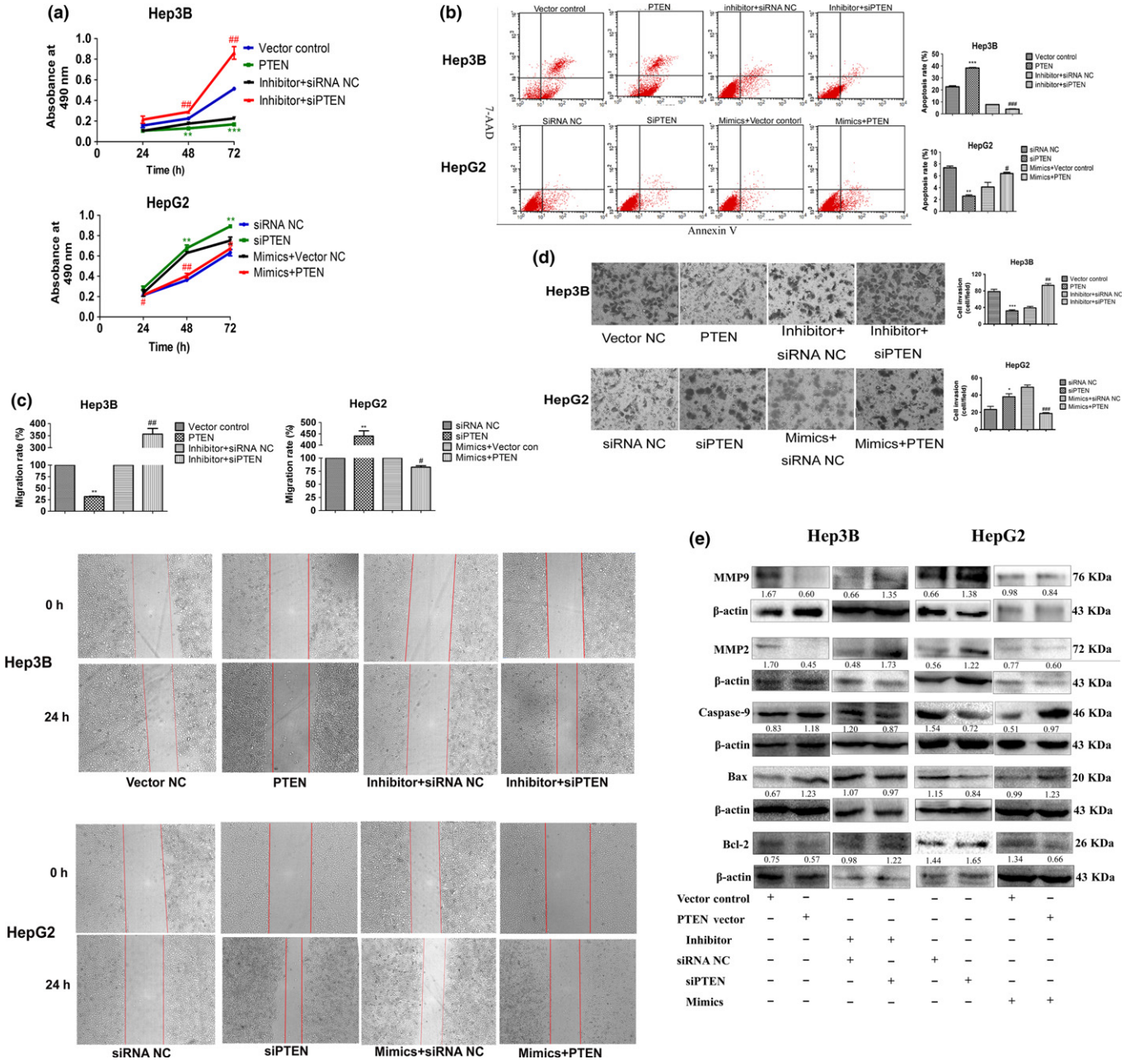

Fig. 4. MiR-155-5p promotes hepatocellular carcinoma (HCC) malignancy through targeting PTEN. (a–e) Cell viability, the percentage of apoptotic cells, wound healing and transwell assays, and the expression of Bcl-2, Bax, caspase-9, MMP2 and MMP9 in Hep3B and HepG2-transfected PTEN plasmid and PTEN siRNA with and without miR-155-5p mimics or inhibitor; the intensity of each band was quantified; the value under each lane indicates the relative expression level of the regulators; n = three repeats with similar results, $^{*}P < 0.05$, $^{**}P < 0.01$, $^{***}P < 0.001$ by Student's t-test, versus inhibitor and mimics NC, respectively. $\#P < 0.05$, $\#\#P < 0.01$, $\#\#\#P < 0.001$ by Student's t-test, versus inhibitor + siRNA NC and mimics + PTEN vector control, respectively. PTEN, PTEN plasmid; siPTEN, PTEN siRNA.

knocking in miR-155-5p in HepG2 cells increased the ability of migration by 119.00% compared with respective control (Fig. 3c). Similarly, downregulating miR-155-5p significantly reduced invasion ability in Hep3B cells (61.67 ± 10.27 and 101.67 ± 4.73 cells/field for miR-155-5p inhibitor and inhibitor NC, respectively; $P < 0.01$), while reexpressing miR-155-5p in HepG2 cells significantly increased invasion ability (59.33 ± 5.86 and 14.00 ± 3.61cells/field for miR-155-5p mimics and mimics NC, respectively; $P < 0.05$, Fig. 3d).

To further understand the mechanisms by which miR-155-5p promoted HCC progression, western blots were used to measure the expression of apoptotic proteins. The results revealed that the expression of Bcl-2 decreased, but the expression of Bax and caspase-9 increased in Hep3B cells transfected with miR-155-5p inhibitor. In contrast, the expression of Bcl-2 increased, but the expression of Bax and caspase-9 decreased in HepG2 cells transfected miR-155-5p mimics. We also determined that MMP2 and MMP9, both of which are correlated with the ability of invasion and migration, were upregulated in HepG2 cells transduced with

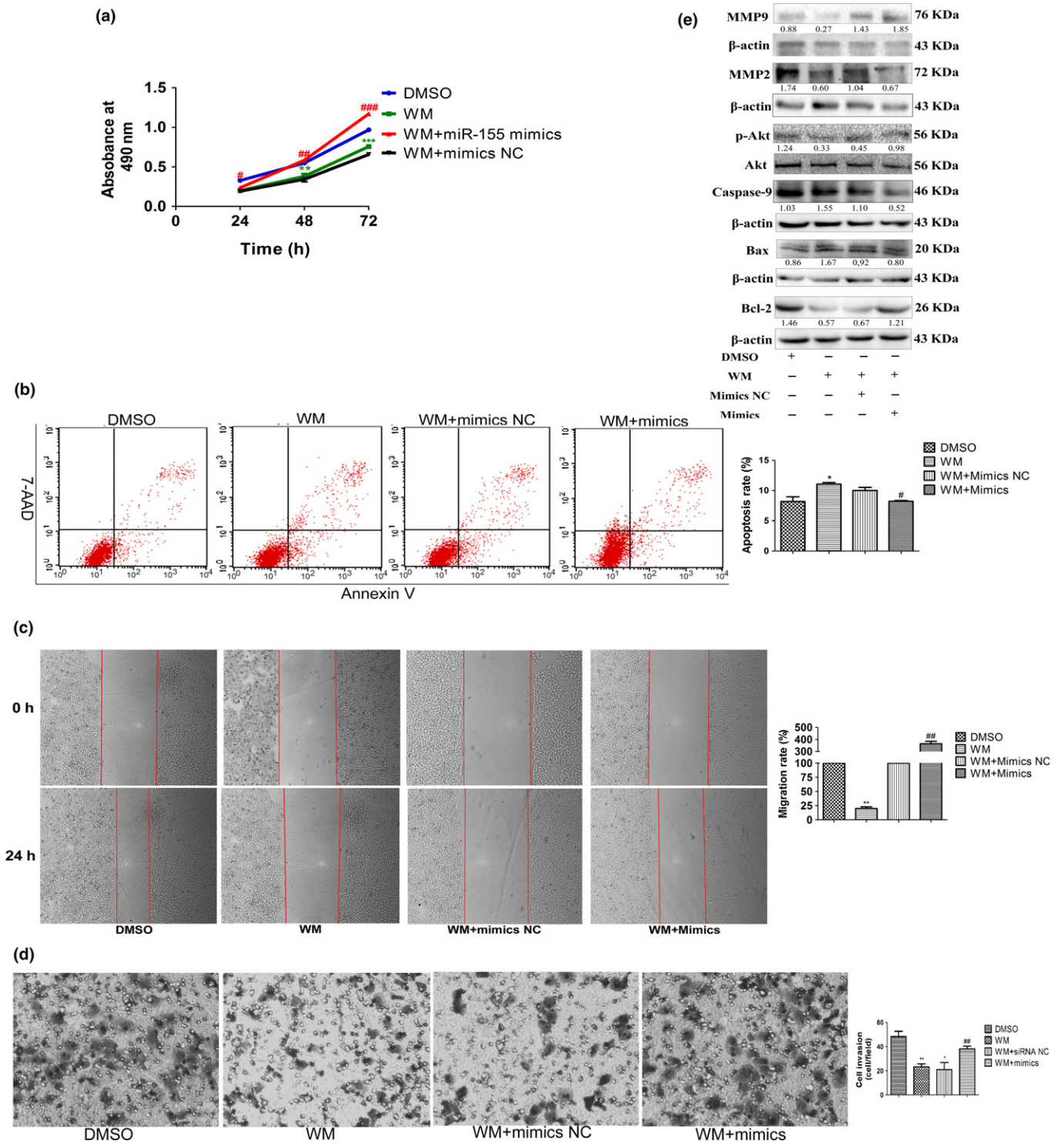

Fig. 5. MiR-155-5p promotes proliferation, invasion and migration, and inhibits apoptosis by the PI3K/Akt pathway. (a–e) Cell viability, the percentage of apoptotic cells, wound healing and transwell assay, and the expression of Akt and p-Akt, Bcl-2, Bax, caspase-9, MMP2 and MMP9 in Hep3B cells treated with DMSO, wortmannin alone, wortmannin and miR mimics NC, and wortmannin and miR-155-5p mimics; the intensity of each band was quantified; the value under each lane indicates the relative expression level of the regulators; n = three repeats with similar results, *$P < 0.05$, **$P < 0.01$, versus Hep3B treated with DMSO; #$P < 0.05$, ##$P < 0.01$, ###$P < 0.001$, versus Hep3B treated with wortmannin alone by Student's t-test. WM, wortmannin.

miR-155-5p mimics, but were downregulated in Hep3B cells transduced with miR-155-5p inhibitor (Fig. 3e). In summary, these results suggested that the ectopic expression of miR-155-5p in HCC cells promoted cell growth, migration and invasion, but inhibited apoptosis *in vitro*.

MiR-155-5p promotes proliferation, migration, invasion and reduced apoptosis in hepatocellular carcinoma through targeting PTEN. To further confirm that miR-155-5p plays an oncogenic role in HCC by targeting PTEN, we used PTEN plasmid and PTEN siRNA to perform gain- and loss-of-function

experiments, and the results showed that similar to miR-155-5p inhibitor, PTEN plasmid significantly reduced proliferation in Hep3B cells by 73.2%, but siPTEN significantly enhanced proliferation in HepG2 cells by 41.5% at 48h post-transfected ($P < 0.05$; Fig. 4a). Moreover, siPTEN could rescue the inhibitory effects on cell viability caused by miR-155-5p inhibitor by 280.0% in Hep3B cells, whereas PTEN acquisition reversed the effects on proliferation by 35.60% in HepG2 cells transfected with miR-155-5p mimics ($P < 0.01$; Fig. 4a). In addition, the results of flow cytometric analysis showed that in Hep3B cells, PTEN plasmid increased the apoptosis rate from 22.67 ± 1.51% (when transducing vector control) to 38.29 ± 0.82% (when transducing PTEN plasmid, $P < 0.001$); however, in HepG2 cells, the apoptosis rate changed from 7.36 ± 0.49% (when transducing siRNA NC) to 2.57 ± 0.36% (when transducing siPTEN, $P < 0.001$). PTEN suppression decreased the apoptosis rate in Hep3B cells transfecting miR-155-5p inhibitor from 7.81 ± 0.24% (when transducing miR-155-5p inhibitor and siRNA NC) to 3.99 ± 0.36% (when transducing miR-155-5p inhibitor and siPTEN; $P < 0.001$); in contrast, PTEN acquisition increased the apoptosis rate in HepG2 cells transfecting miR-155-5p mimics from 4.10 ± 1.37% (when transducing miR-155-5p mimics and vector control) to 6.39 ± 0.31% (when transducing miR-155-5p mimics and PTEN plasmid; $P < 0.05$; Fig. 4b).

Next, we used wound healing and transwell assays to examine the ability of migration and invasion after inducing PTEN. We noticed that similar to miR-155-5p inhibitor, in Hep3B cells, PTEN overexpression impaired the ability of migration by 31.67%; but PTEN downexpression could reverse the suppression of migration ability caused by inhibitor by 356.67%; in HepG2 cells, siPTEN enhanced migration by 440%, but PTEN overexpression rescued the effects led by mimics by 82.67% (Fig. 4c). Similar results were observed in transwell assay: Hep3B cells invasion ability was suppressed when transducing PTEN plasmid (78.67 ± 9.02 cells/field for PTEN, 32.00 ± 4.58 cells/field for vector control, $P < 0.01$), but rescued when transducing siPTEN together with inhibitor (39.00 ± 6.56 cells/filed for siPTEN + inhibitor, 93.33 ± 7.57 cells/filed for siRNA NC + inhibitor, $P < 0.01$; Fig. 4d) and vice versa in HepG2 cells.

Finally, western blots were carried out to measure the expression of apoptotic proteins and MMP. The results revealed that the expression of Bcl-2 decreased, but the expression of Bax and caspase-9 increased when transfecting PTEN plasmid in Hep3B cells. In contrast, the expression of Bcl-2 increased, but the expression of Bax and caspase-9 decreased when transfecting PTEN siRNA in HepG2 cells. Moreover, reduction of PTEN expression in Hep3B cells transfected with miR-155-5p inhibitor reversed the expression of Bcl-2, Bax and caspase-9 compared with transfecting with miR-155-5p inhibitor and siRNA NC; however, re-expressing PTEN in HepG2 cells transfected with miR-155-5p mimics mitigated the expression of Bcl-2, Bax and caspase-9, compared with transducing miR-155-5p mimics and PTEN vector control. We

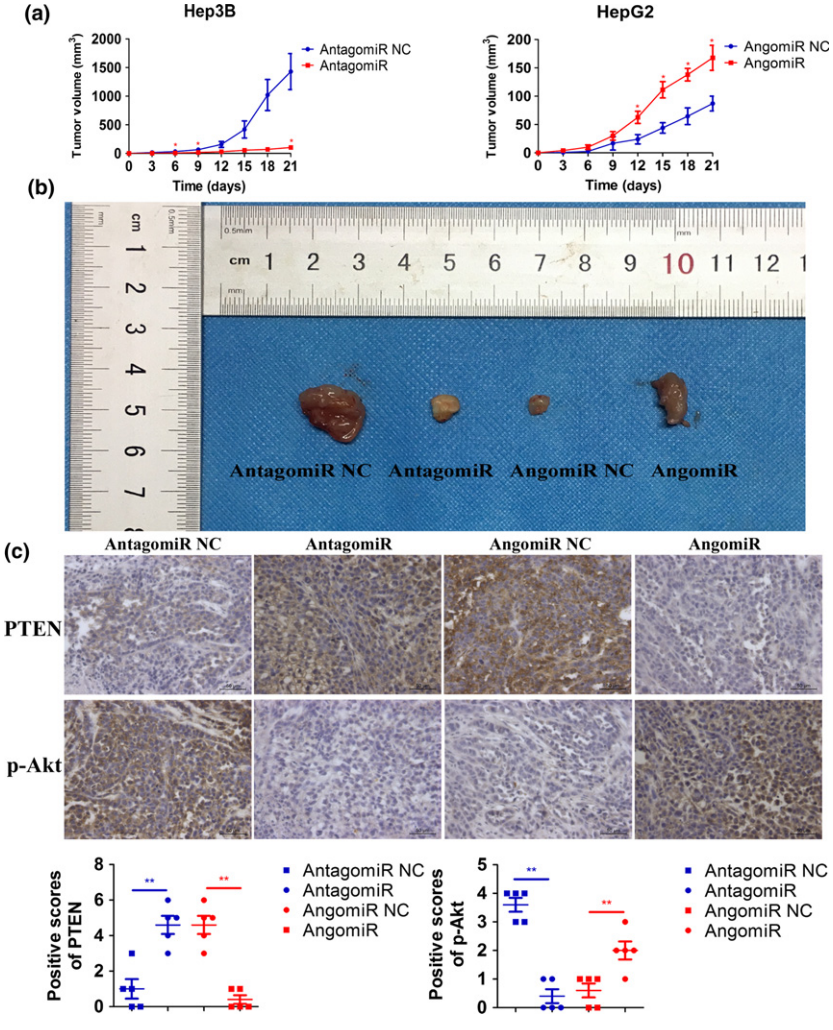

Fig. 6. MiR-155-5p promotes HCC progression *in vivo*. (a) Growth curves of Hep3B and HepG2 cell line xenograft tumors after injection with miR-155-5p antagomiR and miR-155-5p angomiR, respectively. Tumor volumes are showed as mean SD for each goup of six mice. (b) BALB/c nude mice resected tumors from each group are shown. (c) The top panel shows representative pictures of PTEN and p-Akt expression in the tissues resected from mice injected Hep3B with antagomiR or antagomiR NC, or HepG2 with angomiR or angomiR NC. The bottom panel shows positive scores of PTEN and p-Akt expression in the implanted tumors resected from mice injected Hep3B with antagomiR or antagomiR NC, or HepG2 angomiR or angomiR NC. *$P < 0.05$, **$P < 0.01$, versus antagomiR NC and angomiR NC, respectively, by Student's *t*-test.

also determined that MMP2 and MMP9 were downregulated in Hep3B cells transduced with PTEN plasmid, but upregulated in HepG2 transfected with PTEN siRNA. Such phenomena could be reversed through co-transfecting miR-155-5p inhibitor and PTEN siRNA, or miR-155-5p mimics and PTEN plasmid (Fig. 4e). Thus, our data revealed that miR-155-5p exerted an oncogenic role in HCC through targeting PTEN.

MiR-155-5p promotes proliferation, invasion and migration, and inhibits apoptosis by the PI3K/Akt pathway. Because PTEN is the main tumor suppressor of the PI3K/Akt pathway, we next studied the effect of the miR-155-5p on PI3K/Akt pathway activation. Treatment with wortmannin (WM) at 200 nmol/mL after 30 min in Hep3B cells[25] showed a significant decrease in p-Akt levels. However, the expression of p-Akt was increased by miR-155-5p mimics (Fig. 5e), indicating that miR-155-5p affected the PI3K/Akt pathway. WM alone decreased the growth rate by 30.5% ($P < 0.01$; Fig. 5a), the migration rate by 20.0% ($P < 0.01$; Fig. 5c), compared with DMSO treatment, and reduced the number of invasive cells from 48.33 ± 7.64 cells/field (DMSO treated) to 23.33 ± 4.16 cells/field (WM-treated; $P < 0.01$; Fig. 5d) but enhanced the apoptosis rate from 8.18 ± 1.36% (DMSO-treated) to 11.1 ± 0.42% (WM-treated; $P < 0.05$; Fig. 5b). Moreover, the results of western blots agreed with the functional experiments. Thus, we concluded that WM could repress tumorigenesis in Hep3B cells by reducing the activity of the PI3K/Akt pathway.

Transfection of miR-155-5p mimics after administration of WM in Hep3B cells increased cell viability by 70.5% compared with cells treated with WM and miR mimics NC ($P < 0.01$; Fig. 5a). In addition, miR-155-5p mimics also reversed the intensive effects caused by WM on apoptosis (10.00 ± 0.92% and 8.21 ± 0.25% for miR mimics NC and WM-treated, miR-155-5p mimics and WM-treated, respectively, $P < 0.05$; Fig. 5b). In accordance with the results of flow cytometry, the expressions of Bcl-2, Bax and caspase-9 were recovered when miR-155-5p was overexpressed after using WM (Fig. 5e). Moreover, WM-treated Hep3B cells regained the abilities of invasion and migration after transfection of miR-155-5p mimics (Fig. 5c, d). The expressions of MMP2 and MMP9 also rose (Fig. 5e). Altogether, these results confirmed that miR-155-5p induced HCC malignancy through the PI3K/Akt pathway.

MiR-155-5p promotes hepatocellular carcinoma progression *in vivo*. We finally tested the oncogenic role of miR-155-5p in BALB/c nude mice through using antagomiR to downregulate miR-155-5p and angomiR to upregulate miR-155-5p. After 3 weeks of observation, the injection of antagomiR showed potent tumor growth inhibition, whereas angomiR showed increased tumor growth (Fig. 6a,b). After confirming that angomiR elevated but antagomiR repressed the expression of miR-155-5p (Fig. S2), we then determined the expression of PTEN and p-Akt in xenografted tumors by immunochemistry; the results showed that PTEN was upregulated while p-Akt was downregulated in the subcutaneous model of Hep3B cell line intratumorally-injected antagomiR; in contrast, PTEN was downregulated while p-Akt was upregulated in xenografted tumors of HepG2 cell line intratumorally injected angomiR (Fig. 6c). Taking these results together, we propose that miR-155-5p also promoted HCC progression *in vivo* through targeting PTEN and activating the PI3K/Akt pathway.

Discussion

Previously, we showed that PTEN regulated angiogenesis and VEGF expression through phosphatase-dependent and -independent mechanisms.[6] We also found that PTEN inhibited migration and invasion of HepG2 cells by decreasing MMP expression via the PI3K/Akt pathway.[7] However, genetic loss or mutation of PTEN rarely occurs in HCC, whereas haploinsufficiency of PTEN, resulting in reduced PTEN expression, has been observed in 32%–44% of HCC patients.[26] Among the various regulations and control factors of mRNA translation, miRs have emerged as a major class of gene expression regulators linked to most biological functions. MiRs are key molecules that alter gene expression post-transcriptionally, leading to silence or subtle decreases of their target genes.[9]

It has been predicted through three bioinformatics tools (Target Scan, DIANA and MicroRNA org) that miR-155-5p has binding sequences for PTEN 3′-UTR. In the current study, we aimed to determine whether miR-155-5p could promote HCC progression through suppressing PTEN. MiR-155-5p was originally been identified as an oncogene,[20–22,27,28] encoded within a region known as B cell integration cluster (Bic) gene.[19]

In the present study, we observed that miR-155-5p upregulation was concurrent with PTEN mRNA downregulation in the DEN-induced rat model, with similar results in human HCC tissues and cell lines. Then we used a dual luciferase reporter gene assay to verify that miR-155-5p directly targeted PTEN 3′-UTR. Next, the dosage-dependent increase or decrease of PTEN in mRNA and protein levels according to miR-155-5p inhibitor or mimics transfection further confirmed that miR-155-5p targeted PTEN 3′-UTR. We also conducted rescue experiments by transfecting PTEN siRNA to Hep3B cells treated with miR-155-5p inhibitor, or transfecting PTEN vector to HepG2 cells treated with miR-155-5p mimics to better illustrate the correlation between miR-155-5p and PTEN. All these results lead to the conclusion that miR-155-5p binds to PTEN 3′-UTR, and represses PTEN expression post-transcriptionally.

Gain- and loss-of-function experiments revealed that miR-155-5p promoted proliferation, invasion and migration, but reduced apoptosis in HCC via repression of PTEN and activation of the PI3K/Akt pathway. Western blots were introduced to determine the underlying mechanisms of miR-155-5p in hepatocarcinogenesis. The results indicated that miR-155-5p-PTEN inhibited apoptosis through intrinsic apoptosis[29–31] pathway by reducing the expression of caspase-9 and Bax but increasing the expression of Bcl-2. In addition, miR-155-5p enhanced migration and invasion through upregulating MMP2 and MMP9, which are often detected in solid tumor tissues and are associated with tumor metastasis in many cancers, including HCC.[32]

Wortmannin, the PI3K/Akt pathway inhibitor, was applied to verify the function of miR-155-5p in the PI3K/Akt pathway. WM is the first described PI3K inhibitor with IC50 of 3 nM in a cell-free assay, binds to the p110 catalytic subunit of PI3K and irreversibly inhibits the enzyme.[33] Considering the relatively low IC50 and little selectivity within the PI3K family,

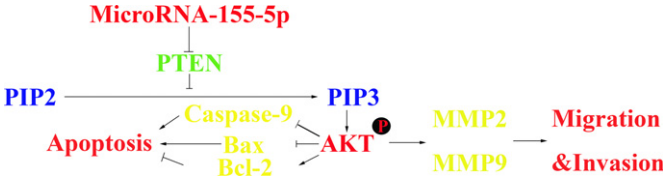

Fig. 7. Schematic diagram of miR-155-5p in promoting HCC progression by suppressing the PTEN via the PI3K/Akt pathway.

WM tends to be better than other PI3K/Akt pathway inhibitors, such as LY294002. Here we utilized WM to suppress the phosphorylation of Akt at ser-473, and, thus, to confirm the role of miR-155-5p in the activation of the PI3K/Akt pathway. The serine/threonine kinase Akt is a highly conserved central regulator of growth-promoting signals in multiple cell types, and inhibition of Akt activity leads to the aberration of cell growth. In our experiments, after confirming that the phosphorylation of Akt was repressed with WM, miR-155-5p mimics were transferred into WM-treated Hep3B cells to rescue the inhibitory effects on the PI3K/Akt pathway caused by WM. MTT, flow cytometry, transwell, wound healing assays and western blots were used to demonstrate that miR-155-5p mimics abolished the inhibitory effects of WM on cell growth, migration and invasion, whereas repressed apoptosis in WM-treated Hep3B cells.

Finally, we established a xenograft tumor model using immunodeficiency mice and demonstrated that miR-155-5p promoted tumorigenesis through targeting PTEN *in vivo*.

The current study revealed that miR-155-5p was correlated with advanced HCC TNM stage, and contributed to HCC malignancy both *in vitro* and *in vivo*. Mechanistically, we demonstrated that miR-155-5p induced HCC cell proliferation, invasion and migration, but inhibited apoptosis by repressing PTEN, which further activated the PI3K/Akt pathway (Fig. 7). Recently, studies have shed light on miR as a novel diagnostic and therapeutic tool. For example, let-7 and miR-34[34] have been considered as important biomarkers for cancer diagnosis, survival and treatment prediction, as well as novel strategies for cancer therapy.[35] The current findings have provided clinical and experimental evidence to support that miR-155-5p plays a vital role in HCC progression, and could be a novel target for HCC diagnosis or therapy.

Acknowledgments

This work was supported by the Natural Science Foundation of China (No. 81301909 and No. 81502099) and the International Cooperation Project in Science and Technology of Shaanxi Province (No. 2016KW-017).

Disclosure Statement

The authors have no conflict of interest to declare.

References

1 Dhanasekaran R, Limaye A, Cabrera R. Hepatocellular carcinoma: current trends in worldwide epidemiology, risk factors, diagnosis, and therapeutics. *Hepat Med* 2012; **4**: 19–37.
2 El-Serag HB. Hepatocellular carcinoma. *N Engl J Med* 2011; **365**: 1118–27.
3 Engelman JA, Luo J, Cantley LC. The evolution of phosphatidylinositol 3-kinases as regulators of growth and metabolism. *Nat Rev Genet* 2006; **7**: 606–19.
4 Li J, Yen C, Liaw D *et al.* PTEN, a putative protein tyrosine phosphatase gene mutated in human brain, breast, and prostate cancer. *Science* 1997; **275**: 1943–7.
5 Salmena L, Carracedo A, Pandolfi PP. Tenets of PTEN tumor suppression. *Cell* 2008; **133**: 403–14.
6 Tian T, Nan KJ, Wang SH *et al.* PTEN regulates angiogenesis and VEGF expression through phosphatase-dependent and -independent mechanisms in HepG2 cells. *Carcinogenesis* 2010; **31**: 1211–19.
7 Tian T, Nan KJ, Guo H *et al.* PTEN inhibits the migration and invasion of HepG2 cells by coordinately decreasing MMP expression via the PI3K/Akt pathway. *Oncol Rep* 2010; **23**: 1593–600.
8 Berger AH, Knudson AG, Pandolfi PP. A continuum model for tumour suppression. *Nature* 2011; **476**: 163–9.
9 Iorio MV, Croce CM. MicroRNAs in cancer: small molecules with a huge impact. *J Clin Oncol* 2009; **27**: 5848–56.
10 Hu R, Kagele DA, Huffaker TB *et al.* miR-155 promotes T follicular helper cell accumulation during chronic, low-grade inflammation. *Immunity* 2014; **41**: 605–19.
11 Costinean S, Zanesi N, Pekarsky Y *et al.* Pre-B cell proliferation and lymphoblastic leukemia/high-grade lymphoma in E(mu)-miR155 transgenic mice. *Proc Natl Acad Sci U S A* 2006; **103**: 7024–9.
12 Wang L, Zhang H, Rodriguez S *et al.* Notch-dependent repression of miR-155 in the bone marrow niche regulates hematopoiesis in an NF-kappaB-dependent manner. *Cell Stem Cell* 2014; **15**: 51–65.
13 Heymans S, Corsten MF, Verhesen W *et al.* Macrophage microRNA-155 promotes cardiac hypertrophy and failure. *Circulation* 2013; **128**: 1420–32.
14 Ferrajoli A, Shanafelt TD, Ivan C *et al.* Prognostic value of miR-155 in individuals with monoclonal B-cell lymphocytosis and patients with B chronic lymphocytic leukemia. *Blood* 2013; **122**: 1891–9.
15 Kong W, He L, Richards EJ *et al.* Upregulation of miRNA-155 promotes tumour angiogenesis by targeting VHL and is associated with poor prognosis and triple-negative breast cancer. *Oncogene* 2014; **33**: 679–89.
16 Jayawardana K, Schramm SJ, Tembe V *et al.* Identification, review and systematic cross-validation of microRNA prognostic signatures in metastatic melanoma. *J Invest Dermatol* 2015; **136**: 245–54.
17 Zhang L, Wang W, Li X *et al.* MicroRNA-155 promotes tumor growth of human hepatocellular carcinoma by targeting ARID2. *Int J Oncol* 2016; **48**: 2425–34.
18 Bhattacharya S, Chalk AM, Ng AJ *et al.* Increased miR-155-5p and reduced miR-148a-3p contribute to the suppression of osteosarcoma cell death. *Oncogene* 2016; **35**: 5282–94.
19 Tam W, Ben-Yehuda D, Hayward WS. bic, a novel gene activated by proviral insertions in avian leukosis virus-induced lymphomas, is likely to function through its noncoding RNA. *Mol Cell Biol* 1997; **17**: 1490–502.
20 Wang B, Majumder S, Nuovo G *et al.* Role of microRNA-155 at early stages of hepatocarcinogenesis induced by choline-deficient and amino acid-defined diet in C57BL/6 mice. *Hepatology* 2009; **50**: 1152–61.
21 Han ZB, Chen HY, Fan JW, Wu JY, Tang HM, Peng ZH. Up-regulation of microRNA-155 promotes cancer cell invasion and predicts poor survival of hepatocellular carcinoma following liver transplantation. *J Cancer Res Clin Oncol* 2012; **138**: 153–61.
22 Ji J, Zheng X, Forgues M *et al.* Identification of microRNAs specific for epithelial cell adhesion molecule-positive tumor cells in hepatocellular carcinoma. *Hepatology* 2015; **62**: 829–40.
23 Guo Hui, Jing Li, Clare FX *et al.* Down-regulation of the cyclin-dependent kinase inhibitor p57 is mediated by Jab1/Csn5 in hepatocarcinogenesis. *Hepatology* 2016; **63**: 898–913.
24 Prieto J. Inflammation, HCC and sex: iL-6 in the centre of the triangle. *J Hepatol* 2008; **48**: 380–1.
25 Chung TW, Lee YC, Ko JH, Kim CH. Hepatitis B Virus X protein modulates the expression of PTEN by inhibiting the function of p53, a transcriptional activator in liver cells. *Cancer Res* 2003; **63**: 3453–8.
26 Augello G, Puleio R, Emma MR *et al.* A PTEN inhibitor displays preclinical activity against hepatocarcinoma cells. *Cell Cycle* 2016; **15**: 573–83.
27 Kasinski AL, Slack FJ. Epigenetics and genetics. MicroRNAs en route to the clinic: progress in validating and targeting microRNAs for cancer therapy. *Nat Rev Cancer* 2011; **11**: 849–64.
28 Yan XL, Jia YL, Chen L *et al.* Hepatocellular carcinoma-associated mesenchymal stem cells promote hepatocarcinoma progression: role of the S100A4-miR155-SOCS1-MMP9 axis. *Hepatology* 2013; **57**: 2274–86.
29 Adams JM, Cory S. The Bcl-2 protein family: arbiters of cell survival. *Science* 1998; **281**: 1322–6.
30 Kluck RM, Bossy-Wetzel E, Green DR, Newmeyer DD. The release of cytochrome c from mitochondria: a primary site for Bcl-2 regulation of apoptosis. *Science* 1997; **275**: 1132–6.
31 Jurgensmeier JM, Xie Z, Deveraux Q, Ellerby L, Bredesen D, Reed JC. Bax directly induces release of cytochrome c from isolated mitochondria. *Proc Natl Acad Sci U S A* 1998; **95**: 4997–5002.
32 Komiya Y, Kurabe N, Katagiri K *et al.* A novel binding factor of 14-3-3beta functions as a transcriptional repressor and promotes anchorage-independent growth, tumorigenicity, and metastasis. *J Biol Chem* 2008; **283**: 18753–64.
33 Zhang F, Zhang T, Jiang T *et al.* Wortmannin potentiates roscovitine-induced growth inhibition in human solid tumor cells by repressing PI3K/Akt pathway. *Cancer Lett* 2009; **286**: 232–9.

34 Trang P, Wiggins JF, Daige CL *et al.* Systemic delivery of tumor suppressor microRNA mimics using a neutral lipid emulsion inhibits lung tumors in mice. *Mol Ther* 2011; **19**: 1116–22.

35 Corsini LR, Bronte G, Terrasi M *et al.* The role of microRNAs in cancer: diagnostic and prognostic biomarkers and targets of therapies. *Expert Opin Ther Targets* 2012; **16**(Suppl 2): S103–9.

Supporting Information

Additional Supporting Information may be found online in the supporting information tab for this article:

Fig. S1. Expression of the miR-155-5p inhibitor and mimics NC-FAM via fluoroscope 24 h after transfection. (a) Expression of the miR-155-5p inhibitor NC-FAM in Hep3B cells via fluoroscope 24 h after transfection. (b) Expression of the miR-155-5p mimics NC-FAM in HepG2 cells via fluoroscope 24 h after transfection.

Fig. S2. Expression of the miR-155-5p in xenograft tumors. The expression of miR-155-5p in xenograft tumors after injecting antagomiR NC, antagomiR, angomiR NC, and angomiR; $*P < 0.05$, versus antagomiR NC, $\#P < 0.05$, versus angomiR NC, by Student's *t*-test.